Strength Softening and Stress Relaxation of Nanostructured Materials

G.J. FAN, H. CHOO, P.K. LIAW, and E.J. LAVERNIA

A composite model is proposed to rationalize the phenomena of strength softening with decreasing grain size for nanostructured materials, which is assumed to consist of a grain interior and an amorphous grain-boundary layer. The grain interior deforms elastically under external stresses, while the linear viscoelastic flow is responsible for the plastic deformation of the grain-boundary layer, whose stress "relaxation" follows Maxwell's equation. The results indicate that the strength of a nanostructured material decreases linearly with decreasing grain size, when the grain size is below a certain threshold. The model is compared with the experimental data from the published studies on nanostructured Cu and Ni. The relevant creep mechanisms for nanostructured materials are also discussed in light of model predictions.

I. INTRODUCTION

IT has long been accepted that dislocations emitted from Frank–Read sources and/or grain boundaries are the carriers for the plastic deformation of coarse-grained polycrystalline materials.[1,2] When a dislocation slips from the grain interior to the grain boundaries, the grain boundaries with a high-angle orientation will stop the dislocation from traveling across them, since crystallographic factors will not allow the dislocation transmission from one grain to an adjacent one through the grain boundary. This process will lead to dislocation pileups at grain boundaries, which embodies the well-known pileup mechanism for the plastic deformation of polycrystalline materials. In this framework, the presence of grain boundaries can effectively strengthen a material by hindering the dislocation motion, and the grain boundary itself is the source for the dislocation nucleation. On the basis of this dislocation pileup mechanism, the flow strength (σ) of a material is inversely proportional to the square root of the grain size (d), *i.e.*,

$$\sigma = \sigma_0 + kd^{-1/2} \qquad [1]$$

where σ_0 and k are material constants. Equation [1] is the well-known Hall–Petch relation,[3,4] which was found to hold for a wide range of polycrystalline materials with grain sizes ranging from a millimeter down to the submicrometer range.

Recently, the applicability of Eq. [1] in the case of nanocrystalline (NC) materials (*e.g.*, grain sizes typically less than 100 nm) has raised some interesting questions, given the fact that in this regime, the grain size is comparable to the grain-boundary width (w).[5,6] There are several reasons that may be used to argue that Eq. [1] may not be valid in the case of NC materials. First, the size of a Frank–Read source for the dislocation nucleation would become larger than the grain size, when the grain size is reduced to a nanometer scale, implying that the accumulation of dislocations would become difficult for NC materials.[7]

G.J. FAN, Researcher, H. CHOO, Assistant Professor, and P.K. LIAW, Professor, are with the Department of Materials Science and Engineering, University of Tennessee, Knoxville, TN 37516. Contact e-mail: gfan@utk.edu E.J. LAVERNIA, Professor, is with the University of California, Davis, CA 95616.

Manuscript submitted January 27, 2005.

In contrast to coarse-grained polycrystals, dislocations are, therefore, source-limited for NC materials, implying that dislocation pileups at grain boundaries are unlikely in the case of NC materials. Published experimental results have already indicated a deviation from the Hall–Petch relation with a relatively lower k value in Eq. [1], when the grain sizes are reduced from the micrometer to nanometer range.[8,9,10] Second, when the grain size is comparable to the grain-boundary width, the grain-boundary contribution to the overall plasticity needs to be taken into account, which is typically safely neglected in the case of coarse-grained polycrystals. Finally, the obvious limitation of Eq. [1] stems from the obvious physical limitation that the strength of NC materials cannot increase infinitely when the grain size is reduced.

On the basis of the previous discussions, an inverse Hall–Petch relation was presented when the grain size was below a certain threshold (d_c).[11] Therefore, other deformation mechanisms, rather than the dislocation-mediated plasticity, should dominate the plastic deformation of a NC material. Molecular-dynamics simulations have clearly demonstrated a breakdown of the Hall–Petch relation for NC materials due to the increased grain-boundary activity during plastic deformation.[12,13,14] It was reported that the yield strength of a NC Cu peaks at a grain size of 10 to 15 nm and decreases with a further decrease of the grain size.[13]

However, the study of the available literature reveals that controversial experimental results have been reported regarding the inverse Hall–Petch relation. These controversial results may be due to several reasons, including sample flaws and contaminations.[15,16] Moreover, there is a distribution of grain sizes for NC materials, and the determination of the grain size for a NC material is not a straightforward exercise. For example, there is a discrepancy for grain sizes determined by the X-ray diffractometer (XRD) and transmission electron microscope (TEM).[17] Despite these difficulties in obtaining reproducible mechanical-property data for NC materials, the presence of an inverse Hall–Petch relation has been confirmed by different groups for the NC Cu, Ni, *etc.*[18–21]

To explain the observed inverse Hall–Petch relation for NC materials, different models have been proposed.[11,18,22–31] A number of investigators have suggested that the inverse Hall–Petch relation can be attributed to the increased grain-boundary activity due to grain-boundary sliding and/or the

diffusional mass transfer *via* grain-boundary diffusion. For example, Masumura *et al*. suggested that the strength softening with decreasing grain size is due to the competition between the conventional dislocation motion and grain-boundary diffusion *via* the Coble creep,[29] which is assumed to be responsible for the room-temperature plastic deformation of NC materials. However, it is not clear that the Coble creep,[32] which successfully describes the creep mechanism of coarse-grained polycrystals, can be extended to NC materials with grain sizes of several nanometers. Moreover, the experimental data indicate a mild grain-size dependence of the yield strength in the strength-softening region,[18] in contrast to a very strong grain-size dependence, as required by the Coble creep. Following the work by Masumura *et al*., Fedorov *et al*. took the triple-junction diffusional creep into account to explain the grain-size dependence of the yield strength of NC materials.[31] Scattergood and Koch proposed a line-tension model based on the dislocation motion, which is assumed to be responsible for the plastic deformation over the entire range of grain sizes.[22] They reported that strength softening with decreasing grain size occurs in a NC material when the grain size is comparable to the cut-off distance for the stress field of dislocations.[22]

The Inverse Hall–Petch relation for the NC materials can also be interpreted using a composite model.[23,26,28–31,33,34] A review of the composite model was given by Gutkin *et al*.[34] In the present investigation, a composite model is proposed using a different approach. It is assumed that a grain-boundary layer having an amorphous structure will deform viscoelastically during plastic deformation in a NC material. The stress relaxation of the grain-boundary layer follows Maxwell's equation. The creep mechanisms of coarse-grained polycrystals have been well established. In this work, we develop a formula to describe the steady-creep rate of NC materials, predicting a relatively weak grain-size dependence, compared with those predicted by the Coble creep[32] and Nabarro–Herring creep.[35,36]

II. MODEL DEVELOPMENT

We assume that a NC material with a grain size of d consists of a mixture of a crystalline grain interior, which is free from dislocations, and a grain-boundary layer having a width of w (Figure 1). The grain-boundary width is approximately 3 times the Burgers vector (**b**), *i.e*., $w \cong 3\mathbf{b}$. The volume fraction of the grain-boundary layer (f) can be expressed by

$$f = \frac{g_1(d/2)^3 - g_1(d/2 - w/2)^3}{g_1(d/2)^3} = 1 - \left(1 - \frac{w}{d}\right)^3 \quad [2]$$

with g_1 defined as a constant whose value depends on the grain morphology. For a spherical grain, g_1 is $4\pi/3$. The calculated volume fraction of the grain-boundary layer as a function of the grain size is shown in Figure 2 in the case of the NC Cu. The volume fraction of the grain-boundary layer increases very rapidly with decreasing grain size when the grain size is less than 40 nm. For example, the volume fraction of the grain-boundary layer amounts to about 20 pct for the NC Cu with a grain size of 15 nm. Therefore, the contributions due to the grain-boundary layer to the overall plasticity need to be taken into account for NC materials. It is

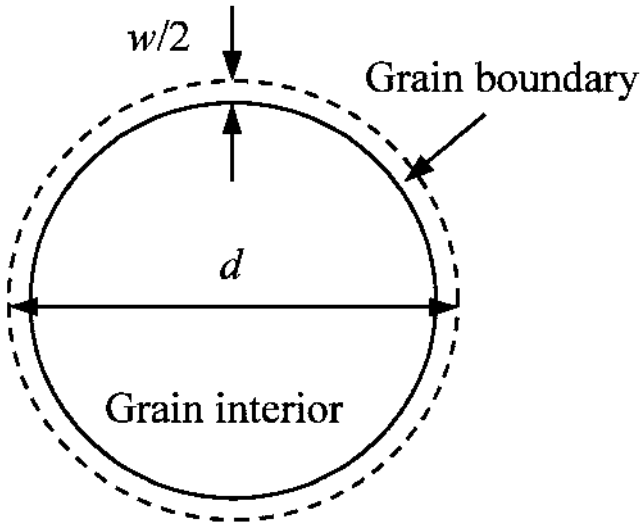

Fig. 1—A grain with a size of d, consisting of the grain interior and a grain-boundary layer with a width of w.

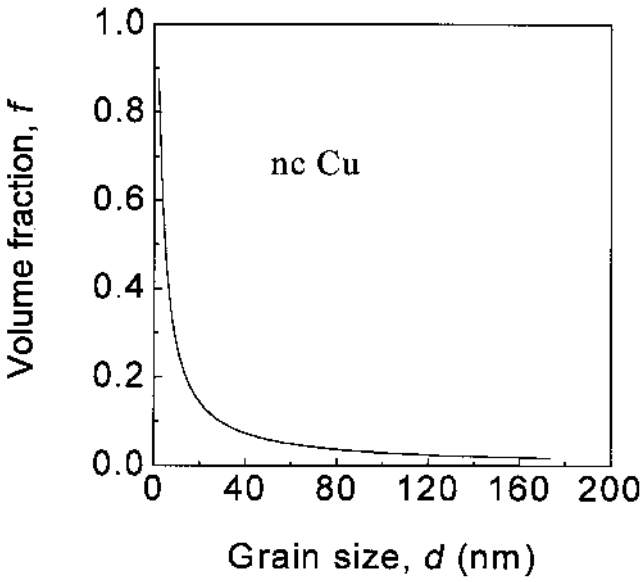

Fig. 2—Volume fraction of the grain-boundary layer as a function of grain size for a NC Cu.

assumed that the flow equations of a NC material consisting of a crystalline grain interior (denoted by l) and a grain-boundary layer (denoted by b) follow a simple rule of mixtures, *i.e*.,

$$\sigma = (1 - f)\,\sigma_l + f\sigma_b \quad [3]$$

$$\varepsilon = (1 - f)\,\varepsilon_l + f\varepsilon_b \quad [4]$$

where σ, σ_l, and σ_b (or ε, ε_l, and ε_b) are the stresses (or strains) of a NC material, crystalline grain interior, and grain-boundary layer, respectively. When $\sigma = \sigma_l = \sigma_b$, the previous equations reduce to the equal-stress condition of the composite materials, while these two equations reduce to the equal-strain condition if $\varepsilon = \varepsilon_l = \varepsilon_b$. The derivative of

Eqs. [3] and [4] with respect to time (t) lead to the stress rate ($\dot{\sigma}$) and strain rate ($\dot{\varepsilon}$) of the NC material expressed by the respective components of the grain interior and grain boundary, *i.e.*,

$$\dot{\sigma} = (1 - f)\,\dot{\sigma}_l + f\dot{\sigma}_b \quad [5]$$

$$\dot{\varepsilon} = (1 - f)\,\dot{\varepsilon}_l + f\dot{\varepsilon}_b \quad [6]$$

The structure of grain boundaries in NC materials remains a topic of active investigations.[5–7,12–14,20,37–45] Both high-resolution TEM and computer simulations have been used to obtain the structural information of grain boundaries in NC materials. Despite tremendous efforts to clarify the structure of NC materials, this issue is still under active debate.

One of the theories regarding the structure of grain boundaries is that the grain boundary is composed of a layer of an amorphous phase with disordered atomic arrangements. Using the molecular-dynamics simulation, Keblinski *et al.* concluded that grain boundaries in NC Pd and Si with high-energy bicrystalline grain boundaries consist of a glassy, gluelike, intergranular phase.[44,45] Many NC materials are binary alloys or pure elemental metals. Amorphous alloys in binary systems were frequently reported, even in some immiscible systems, such as Ag-Ni[46] and Ni-W.[20] Despite the fact that the formation of amorphous pure metals is kinetically unfavorable, compared with binary and multicomponent alloy systems, the existence of an amorphous state in pure metals has already been confirmed both experimentally and theoretically.[17,47–52] In the current work, the grain-boundary layer of the NC materials is assumed to be a glassy structure. Due to the simple chemistry of the grain boundary of a NC material with one component, the amorphous layer of grain boundaries is expected to exhibit a much lower reduced glass-transition temperature (T_g/T_m), compared to the multicomponent metallic glasses (T_g is the glass-transition temperature and T_m is the melting point).[53] Fecht and Johnson predict that the glass-transition temperature for pure elements is only $0.25T_m$.[17] Applying this relation to the amorphous Cu leads to a T_g value of 340 K, which is comparable with the value obtained by computer simulations.[51,52]

Due to a low glass-transition temperature (close to or even lower than room temperature), the plastic deformation of amorphous metals and alloys with a simple chemistry may show a viscoelastic flow at room temperature. A nonlinear viscoplastic deformation at the grain boundary for the NC materials was assumed by Van Swygenhoven and Caro.[53] Here, we assume that a viscoelastic deformation is responsible for the plastic deformation in the amorphous grain-boundary layer. The plastic deformation of a viscoelastic solid is described by a differential constitutive equation, based on a Maxwell model, which has been proven to be very useful when rationalizing the "stress relaxation" of a viscoelastic solid with a single characteristic relaxation time,[54,55] *i.e.*,

$$\dot{\sigma}_b = E_b\dot{\varepsilon}_b - \frac{\sigma_b}{t_b} \quad [7]$$

where $\dot{\sigma}_b$, E_b, $\dot{\varepsilon}_b$, and t_b are the stress rate, Young's modulus, strain rate, and relaxation time of the grain-boundary layer, respectively. For the NC materials, the root-mean-square (RMS) strains always exist. In the present model, the RMS strain can be relaxed during the grain-boundary relaxation.

In the following text, some assumptions were made to solve Eq. [7]. Since the crystalline-grain interior is free from dislocations, we assume an elastic deformation for the grain interior during plastic deformation. When a NC material is strained, a shear stress (τ_b) must be developed between the interfaces of the grain interior and the grain-boundary layer in order to avoid the debonding of the interfaces. Accordingly, a normal stress in the grain interior (σ_l) is built up, which is transmitted from the grain boundary to the grain interior by means of the shear stress (τ_b). The relationship between σ_l and τ_b can be expressed by (refer to the Appendix):

$$\sigma_l = g_2\tau_b \quad [8]$$

with g_2 being the geometric factor depending on the shape of the grain. The Newtonian viscosity of the grain-boundary layer, *i.e.*, η_b, is determined by the normal stress (σ_b) and the strain rate ($\dot{\varepsilon}_b$):

$$\eta_b = \frac{\sigma_b}{3\dot{\varepsilon}_b} \quad [9]$$

The shear stress depends not only on the normal stress, but also on its direction. The maximum shear stress is $\tau_b = \sigma_b/2$ for a homogeneous solid. For simplicity, we assume that the shear stress is the same at all directions (refer to the Appendix) and is described by

$$\tau_b = g_3\sigma_b \quad [10]$$

with g_3 being another geometric factor. For a viscoelastic solid, the relaxation time (t_b) in Eq. [7] is related to the Newtonian viscosity as expressed by

$$\frac{1}{t_b} = \frac{G_b}{\eta_b} \quad [11]$$

where G_b is the shear modulus for the viscoelastic solid. A combination of Eqs. [8] through [11] yields

$$\sigma_l = 3g_2g_3G_bt_b\dot{\varepsilon}_b \quad [12]$$

According to Hooke's law for the elastic solid of the grain interior, the strain of the grain interior (ε_l) is given by $\varepsilon_l = \sigma_l/E_l$. Therefore,

$$\varepsilon_l = \frac{3g_2g_3G_bt_b\dot{\varepsilon}_b}{E_l} \quad [13]$$

Differentiation of Eq. [13] with respect to the time (t) leads to $\dot{\varepsilon}_l = 0$, assuming a constant strain rate. Following Eq. [6], the strain rate of the grain-boundary layer is, therefore, given by

$$\dot{\varepsilon}_b = \frac{\dot{\varepsilon}}{f} \quad [14]$$

Substituting Eq. [12] into [3] arrives at an expression for the normal stress of the grain boundary by

$$\sigma_b = \frac{\sigma - 3(1-f)g_2g_3G_bt_b\dot{\varepsilon}_b}{f} = \frac{\sigma - 3\left(\frac{1}{f} - 1\right)g_2g_3G_bt_b\dot{\varepsilon}}{f} \quad [15]$$

A derivative of σ_b in Eq. [15] with respect to t leads to

$$\dot{\sigma}_b = \frac{\dot{\sigma}}{f} \qquad [16]$$

Equations [5] and [16] imply that the stress rate of the crystalline-grain interior is 0. The previous results indicate that the elastic-grain interior does not have any contributions to the overall strain rate and stress rate, assuming a constant strain rate. The strain rate and stress rate of the grain-boundary layer are equal to those of the NC material divided by the volume fraction of the grain-boundary layer.

Substituting Eqs. [14] through [16] into Eq. [7] leads to the flow equation of a NC material, given as

$$\frac{\dot{\sigma}}{f} = \frac{E_b\dot{\varepsilon}}{f} - \frac{\sigma - 3\left(\frac{1}{f} - 1\right)g_2g_3G_bt_b\dot{\varepsilon}}{t_bf} \qquad [17]$$

In Eq. [17], the shear modulus is approximately one-third of the Young's modulus i.e., $G_b \cong E_b/3$. The solution of Eq. [17] is given as

$$\begin{aligned}\sigma(t) &= 3t_bG_b\dot{\varepsilon}\left[1 + g_2g_3\left(\frac{1}{f} - 1\right)\right]\left[1 - \exp\left(-\frac{t}{t_b}\right)\right] \\ &= 3\eta_b\dot{\varepsilon}\left[1 + g_2g_3\left(\frac{1}{f} - 1\right)\right]\left[1 - \exp\left(-\frac{t}{t_b}\right)\right] \qquad [18]\end{aligned}$$

Equation [18] indicates that the stress relaxation of a NC material is related to the viscosity of the grain boundary, the strain rate, the shape of the grain, as well as the volume fraction of the grain-boundary layer.

The viscosity of the grain-boundary layer (η_b) in Eq. [18] can be linked with the diffusivity by means of a Stokes-Einstein relation,[56,57] *i.e.*,

$$\frac{k_BT}{6\pi R} = D_b\eta_b \qquad [19]$$

where k_B is the Boltzmann constant, T is the absolute temperature, R is the radius of atoms at the grain boundaries, and D_b is the diffusivity of the grain boundary.

$$D_b = D_{b0}\exp\left(-\frac{E_b}{k_BT}\right) \qquad [20]$$

with D_{b0} being the pre-exponential factor and E_b being the activation energy for the grain-boundary diffusion. Therefore, Eq. [18] can be rewritten as

$$\sigma(t) = \frac{k_BT\dot{\varepsilon}}{2\pi RD_b}\left[1 + g_2g_3\left(\frac{1}{f} - 1\right)\right]\left[1 - \exp\left(-\frac{t}{t_b}\right)\right] \qquad [21]$$

Note that experimental and theoretical analyses indicate a breakdown of the Stokes–Einstein relation due to a change in the diffusion mechanism involving the cooperative motion of atoms at low temperatures.[58–61] In this case, the parameter R in Eq. [19] no longer represents the mean atomic radius. As will be shown later, R is determined to be several orders of magnitude smaller than the atomic radius. Clearly, Eq. [21] can be reduced to a flow equation of an amorphous material having the same composition as that of the NC counterpart when $f \to 1$. The term of $1/f$ in Eq. [21] can be simplified to be a linear relationship with d/w, as shown in Figure 3. By taking account of the boundary condition, $d/w = 1$, Eq. [21] is expressed as a function of d/w,

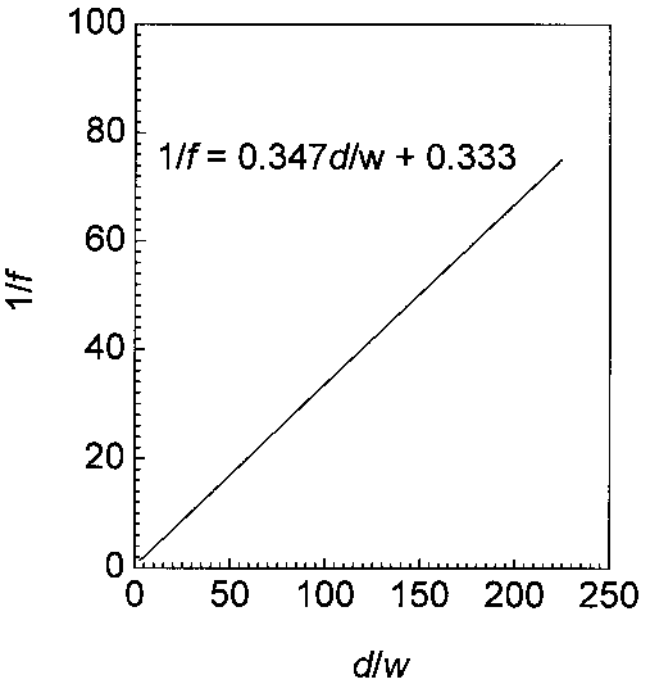

Fig. 3—Inverse volume fraction of the grain-boundary layer, $1/f$, as a function of d/w. The value of $1/f$ shows a linear relation with d/w.

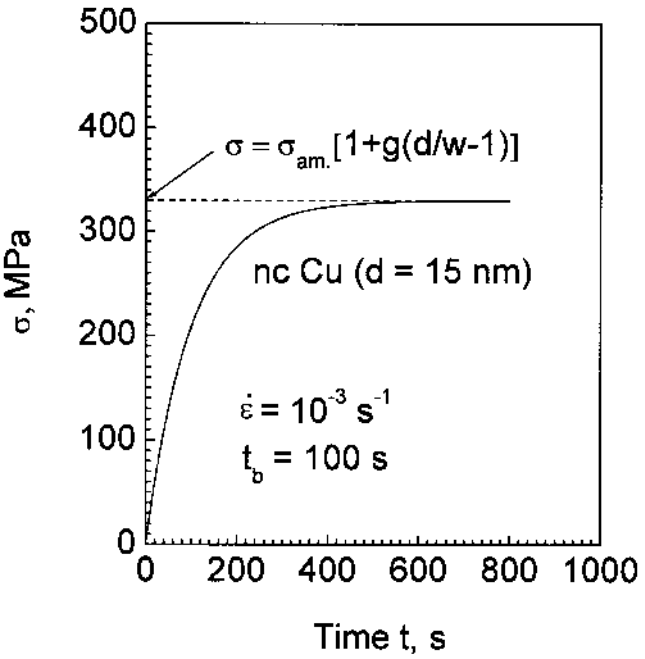

Fig. 4—Stress relaxation of a NC Cu as a function of time.

$$\sigma(t) = \frac{k_BT\dot{\varepsilon}}{2\pi RD_b}\left[1 + g\left(\frac{d}{w} - 1\right)\right]\left[1 - \exp\left(-\frac{t}{t_b}\right)\right] \qquad [22]$$

i.e., where g_2 and g_3 are absorbed into a single geometric factor, g. Figure 4 shows the stress as a function of time for the NC Cu with a grain size of $d = 15$ nm and at a strain rate of

$\dot{\varepsilon} = 10^{-3}\ s^{-1}$. For the calculation in Figure 4, the following values are used for the parameters in Eq. [22]:[62] $T = 300$ K, $R = 1.2 \times 10^{-14}$ m, $D_b = 3 \times 10^{-9}\exp(-0.64eV/k_BT)$, $g = 0.0845$, $w = 3b$ (with $b = 0.25$ nm), and $t_b = 100$ seconds. Figure 4 can be easily converted into a stress-strain curve, since $\varepsilon = \dot{\varepsilon}t$. It is clear that the stress of the NC material reaches a constant value after a sufficient time of the stress relaxation, which ultimately represents the flow strength of a NC material as a function of the grain size, as given by

$$\sigma = \frac{k_BT\dot{\varepsilon}}{2\pi RD_b}\left[1 + g\left(\frac{d}{w} - 1\right)\right] = \sigma_{am.}\left[1 + g\left(\frac{d}{w} - 1\right)\right] \quad [23]$$

Equation [23] shows an inverse Hall–Petch relation, indicating that the strength (σ) of a NC material shows a linear relationship with the grain size, *i.e.*, the strength decreases with decreasing grain size. Equation [23] also suggests that the strength of an amorphous material having the same composition as the NC counterpart is given by $\sigma_{am.} = k_BT\dot{\varepsilon}/2\pi RD_b$, when $d/w = 1$. This equation is the equivalent of Eq. [19], indicating the self-consistence of the model.

III. RESULTS AND DISCUSSION

The grain boundaries for the polycrystals act as sinks and sources for the dislocation activity, which effectively strengthen the materials. The present model predicts that the grain boundaries will soften the NC materials, whereas grain interiors are the strengthening media. The reasons that the grain interiors strengthen the NC materials are twofold. First, a perfect grain interior without dislocations is expected to have a very high strength. It is assumed that the grain interior deforms elastically without yielding during the plastic deformation of NC materials. Second, the grain interior exerts a frictional force on the grain boundary, thereby strengthening the grain-boundary layer. Despite the fact that other deformation mechanisms may also be operative, which may lead to a lower k value in Eq. [1] for the NC materials,[30,63,64] for simplicity, we assume that the plastic deformation in a NC material with a wide range of grain sizes (*e.g.*, from millimeters to nanometers) is a competing process between dislocation pileups at the grain boundaries and grain-boundary activities by means of the grain-boundary relaxation under an external stress.

The experimental data for the NC Cu and Ni have indicated that the Hall–Petch relation essentially holds true, when the grain sizes exceed a certain threshold value (d_c). When $d < d_c$, a breakdown of the Hall–Petch relationship occurs, and the strength softening with decreasing grain size takes place. The present model is applied to fit the experimental data for the NC Cu and Ni. It is assumed that the plastic deformation of a NC material switches abruptly from a dislocation-pileup mechanism to a grain-boundary-relaxation mechanism at a grain size of $d = d_c$, *i.e.*,

$$\sigma_0 + kd_c^{-1/2} = \sigma_{am.}\left[1 + g\left(\frac{d_c}{w} - 1\right)\right] \quad [24]$$

The experimental data of the yield strength of Cu with grain sizes ranging from micrometers to several nanometers are collected in Figure 5. The yield strength of the polycrystalline Cu is somewhat scattered, depending on the sources obtained.

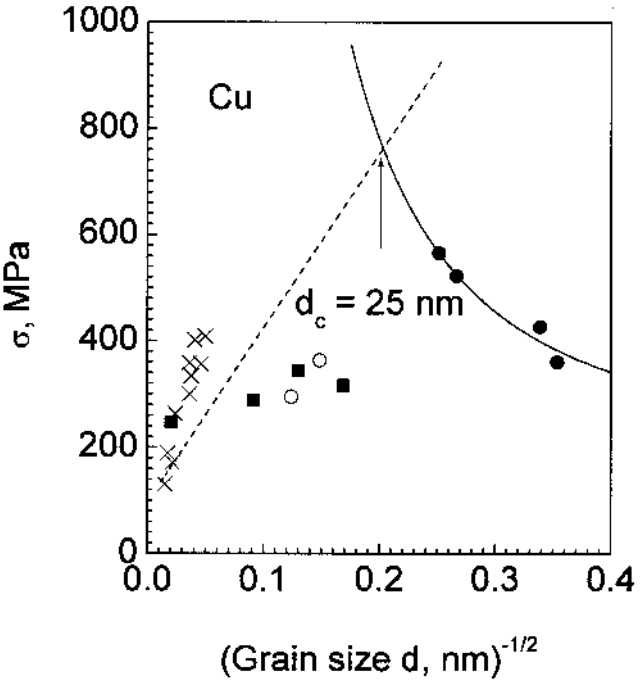

Fig. 5—Yield strength as a function of the inverse square root of the grain size, for Cu. The solid line is a fit to the experimental data using Eq. [22], when $d \le d_c$, while the dashed line is a fit to the experimental data using Eq. [1], when $d > d_c$. The value of $d_c = 25$ nm is determined to be at the crossover (× = data from Ref. 65; ■ = data from Ref. 66; ○ = data from Ref. 67; and ● = data from Ref. 18).

The best fits to the experimental data yield a Hall–Petch relation (Eq. [1]) with $\sigma_0 = 96.7$ MPa and $k = 3{,}273$ MPa nm$^{1/2}$, and an inverse Hall–Petch relation (Eq. [23]) with $\sigma_{am.} = 213$ MPa and a geometric factor of $g = 0.085$. The value of d_c is determined to be 25 nm for the NC Cu, which is relatively larger than the value of 18 nm obtained by Fedorov *et al.*[31] and that of 14 nm obtained by Masumura *et al.*,[29] but smaller than the value of 50 nm obtained by Arzt.[63] The maximum strength of the NC Cu is determined to be $\sigma_{max} = 760$ MPa at a crossover between two fitted curves. The cusp between two curves is not expected experimentally due to the presence of a distribution of grain sizes as well as the smooth transition of the competing deformation mechanisms. The transition will be smooth with a decrease in the grain size from the Hall–Petch relation, based on Eq. [1], to the inverse Hall–Petch relation, based on Eq. [23], if a distribution of grain sizes is taken into account.[29,31]

Figure 6 displays the hardness (H) of the Ni and Ni(W) solid solution. The fitted curves, based on Eqs. [1] and [23], are also included. The hardness is about 3 times the yield stress, *i.e.*, $H = 3\sigma$. A decrease of the hardness with decreasing grain size was observed for the Ni(W) solid solution. Schuh *et al.*[20] have pointed out that the contribution due to the solid-solution strengthening from W is essentially negligible. The hardness between the Ni and Ni(W) can be directly comparable with each other. It is clear that below a certain grain-size threshold, the Hall–Petch relation works fairly well. The best fit to the experimental data yields a Hall–Petch relation with $H_0 = 0.9$ GPa and $k = 19.1$ MPa nm$^{1/2}$. Equation [23] is used to fit the strength-softening region with decreasing grain size, and the grain-boundary width is 0.75 nm for the fitting. The best

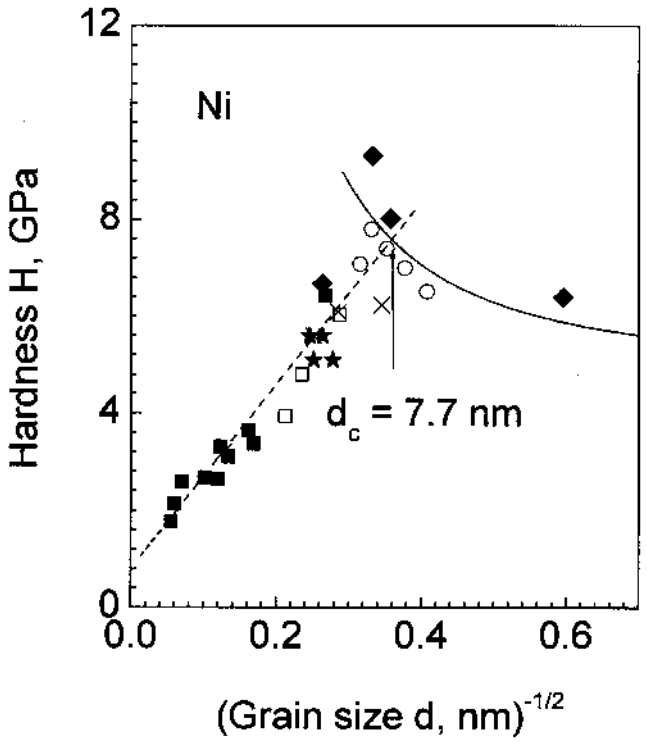

Fig. 6—Hardness as a function of the inverse square root of the grain size, for Ni and Ni(W). The solid line is a fit to the experimental data using Eq. [22], when $d \leq d_c$, while the dashed line is a fit to the experimental data using Eq. [1], when $d > d_c$. The value of d_c = 7.7 nm is determined to be at the crossover (■ = data from Ref. 68; □ = data from Ref. 19; ★ = data from Ref. 69; × = data from Ref. 70; ○ = data from Ref. 20; and ◆ = data from Ref. 71).

fit yields an inverse Hall–Petch relation (Eq. [23]) with $\sigma_{am.}$ = 5.2 GPa and a geometric factor of $g = 0.05$. The value of d_c is determined to be 7.7 nm for the NC Ni, which is comparable with the value of 8 nm found by Schuh *et al.*[20] The hardness of the amorphous Ni obtained through fitting the experimental data, using Eq. [23], is comparable with amorphous Ni-based alloys.[72]

The Nabarro–Herring (N-H) creep and Coble creep have been used to explain the creep mechanisms of polycrystalline materials, which suggest that the diffusion of vacancies through crystal lattices or along the grain boundaries under external stresses is responsible for the flow rate during creep. The N-H creep predicts the steady-creep rate based on the vacancy flow through the crystal lattice:[35,36]

$$\dot{\varepsilon} = \frac{14 D_l \Omega \sigma}{k_B T}\left(\frac{1}{d}\right)^2 \qquad [25]$$

where D_l is the lattice diffusivity, which is described by $D_l = D_{l0} \exp(-E_l/k_B\mathrm{T})$, where D_{l0} is the pre-exponential factor, E_l is the activation energy for the lattice diffusion, and Ω is the atomic volume. The Coble creep predicts the steady-creep rate based on the vacancy flow along the grain boundaries:[35]

$$\dot{\varepsilon} = \frac{148 D_b \Omega w \sigma}{\pi k_B T}\left(\frac{1}{d}\right)^3 \qquad [26]$$

Equations [25] and [26] indicate that the creep rate increases with decreasing grain size, with a grain-size exponent of 2 for the N-H creep and of 3 for the Coble creep. Moreover, the steady-creep rate shows a linear relationship with the stress, characteristic of the Newtonian viscous flow. It is believed that the Coble creep will predominate over the N-H creep at the low temperature and very small grain sizes. Therefore, it is expected that the Coble creep should be responsible for the creep of NC materials. Experimental studies of creep mechanisms of NC materials encounter two major difficulties, which are intrinsic to NC materials. First, NC materials have a large volume fraction of grain boundaries, which is at a high-energy state. To reduce the free energy, NC materials have a strong tendency for the grain growth at a relatively low temperature.[73] Second, the determination of the grain size of a NC material is not straightforward due to a distribution of grain sizes.

Although some experimental data are available in the literature,[9,15,74–78] the experimental creep data of NC materials from different sources are too limited to confirm any of the available creep mechanisms, especially for the relationship between the steady-creep rates and grain sizes. The conventional Coble creep suggests a grain-size exponent of 3 for the steady-creep rate. Recently, Yamakov *et al.*[43] pointed out that the grain-size exponent decreases from 3 to 2 when the width of grain boundaries is comparable with the grain size ($d \approx 2w$). Molecular-dynamic computer simulations indicate that the cubic grain-size dependence of the strain rate demanded by the Coble creep may be overestimated for the NC materials.[37,79,80] A grain-size exponent of 2 or even 1 was obtained in NC materials, in contrast to that of 3 predicted by the conventional Coble creep. Moreover, Ashby[81] and Arzt *et al.*[82] have shown a much weaker grain-size dependence of the steady-creep rate, if the creep of a NC material is controlled by the deposition and removal of atoms at the grain boundaries, rather than by the diffusional step in the Coble creep. These results confirmed a relatively weak grain-size dependence on the steady-creep rate for NC materials.

In the present investigation, following Eq. [23], the steady-creep rate of a NC material with a grain size of d can be expressed as

$$\dot{\varepsilon} = \frac{2\pi D_b R \sigma}{k_B T} \frac{1}{1 + g\left(\frac{d}{w} - 1\right)} \qquad [27]$$

Equation [27] has a similar form, compared with Eqs. [25] and [26], also indicating that the stress exponent is 1. However, the grain-size exponent is less than 1, which depends on the geometric factor, i.e., the shape of the grains. It is assumed that Eq. [27] governs the creep rate of a NC material for the grain size for which $\mathrm{d} \leq d_c$ (d_c is determined by Eq. [24]). Also, Eq. [26], *i.e.*, the Coble creep, is responsible for the creep rate for $\mathrm{d} > d_c$. Then, at $d = d_c$, the following equation holds:

$$\frac{148 D_b \Omega w \sigma}{\pi K_B T}\left(\frac{1}{d_c}\right)^3 = \frac{2\pi D_b R \sigma}{k_B T} \frac{1}{1 + g\left(\frac{d_c}{w} - 1\right)} \qquad [28]$$

Therefore, the Stokes–Einstein constant, R, can be expressed as

$$R = \frac{74 \Omega w}{\pi^2} \frac{1 + g\left(\frac{d_c}{w} - 1\right)}{{d_c}^3} \qquad [29]$$

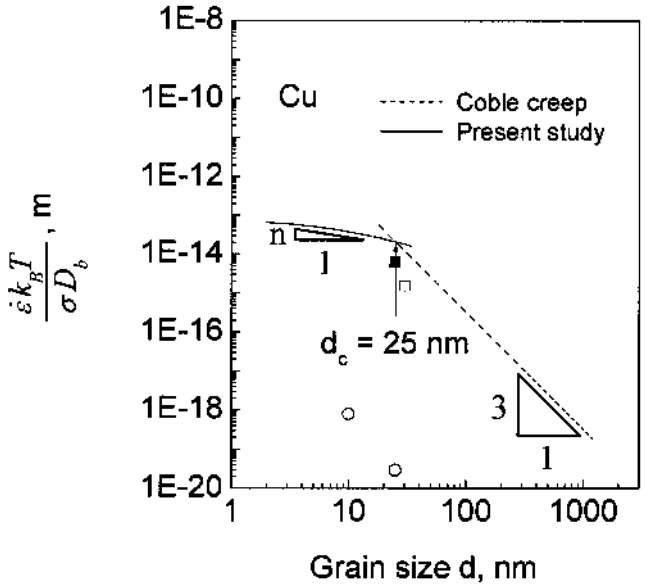

Fig. 7—Normalized steady-creep rate as a function of the grain size, for Cu. The solid line is the calculated value, using Eq. [26], for the present work, and the dashed line is the calculated value, using Eq. [25], for the Coble creep. The Coble creep suggests a grain-size exponent of 3 for $d > d_c$. The grain-size exponent in the present work for $d \leq d_c$ is less than 1. The experimental data are smaller than the predicted values (○ = data from Ref. 83; ■ = data from Ref. 9; and □ = data from Ref. 74).

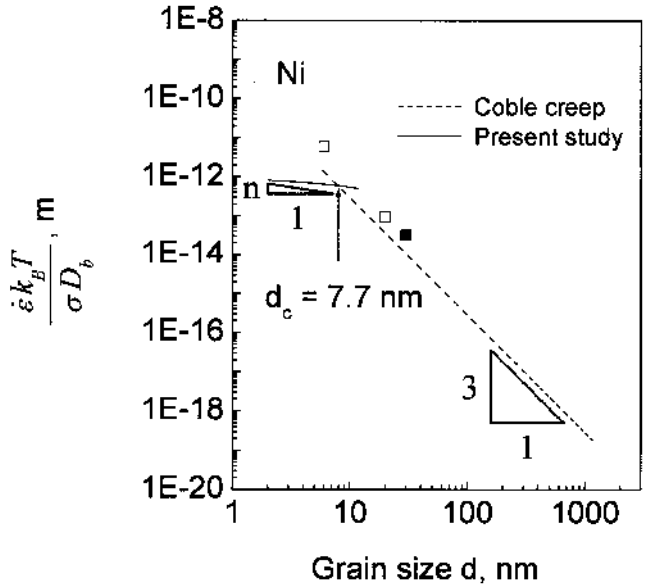

Fig. 8—Normalized steady-creep rate as a function of the grain size, for Ni. The solid line is the calculated value, using Eq. [26], for the present work, and the dashed line is the calculated value, using Eq. [25], for the Coble creep. The experimental data are larger than the predicted values (□ = data from Ref. 75, and ■ = data from Ref. 76).

in which R is determined to be 1.2×10^{-14} m for the NC Cu and 1.4×10^{-13} m for the NC Ni, which is several orders of magnitude smaller than the atomic radius of Cu and Ni, indicating a breakdown of the Stokes–Einstein relation for the NC Cu and Ni. Equations [26] and [27] imply that the steady-strain rates at different temperatures and stress conditions will be cast into a single curve in a $\dot{\varepsilon} k_B T/D_b \sigma \sim d$ plot. Figure 7 shows the calculated $\dot{\varepsilon} k_B T/D_b \sigma$ ratio as a function of the grain size, on a log-log scale. The experimental data from the literature are also included in Figure 7. The following values were used in the calculations:[62] $D_b = 3 \times 10^{-9} \exp(-0.64\text{eV}/k_B T)$ m^2/s and $\Omega = 8.78 \times 10^{-30}$ m^3. Figure 7 indicates that the normalized creep rate is smaller for the present model compared with the Coble creep, when $d \leq d_c$, suggesting that the Coble creep may overestimate the steady-creep rate for the NC materials. The experimental data of the normalized creep rate are smaller than the calculated values. The normalized creep rate as a function of the grain size for the NC Ni is demonstrated in Figure 8. The values of $D_b = 5.3 \times 10^{-6} \exp(-0.89\text{eV}/k_B T)$ m^2/s and $\Omega = 8 \times 10^{-30}$ m^3 are used in the calculations.[84] In this case, the experimental data are larger than the calculated values. Apparently, more experiments are needed to understand the exact creep mechanisms of NC materials. Figures 7 and 8 also suggest that the grain-size exponent for the Coble creep is 3 for $d > d_c$. The grain-size exponents for $d \leq d_c$ are calculated and shown in Figure 9 for the NC Cu and Ni. It was found that the value of the grain-size exponent depends on the grain size and also on the geometric factor. The grain-size exponent of the NC Cu with $g = 0.085$ decreases from 0.76 for $d = d_c = 25$ nm to 0.22 for $d = 2$ nm, while the grain-size exponent of the NC Ni with $g = 0.05$ decreases from 0.37 for $d = d_c = 7.7$ nm to 0.14 for $d = 2$ nm.

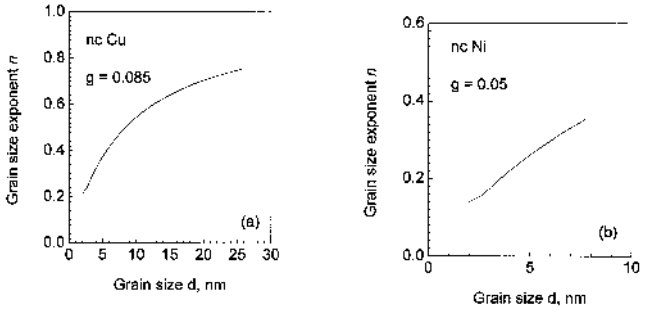

Fig. 9—Grain-size exponent for the steady-state creep of the (*a*) NC Cu and (*b*) NC Ni as a function of the grain size. The value of n depends on the geometric factor, determined from Figs. 5 and 6.

IV. CONCLUSIONS

A theoretical model is proposed in this article to explain the grain-size dependence of the flow strength of NC materials, suggesting a competition between the dislocation slip and grain-boundary activities during the plastic deformation of NC materials. When the grain size is decreased to a critical value, the plastic deformation due to the grain-boundary activities predominates. At the same time, the creep mechanism switches from the Coble creep into a grain-boundary-relaxation mechanism. The model suggests that a NC material consist of an elastic-grain interior, which is free from dislocation activities, and a grain-boundary layer having an amorphous structure. Due to the relatively low glass-transition temperature of the amorphous structure, the grain-boundary layers are assumed to deform viscoelastically at room temperature.

A differential constitutive equation, based on a Maxwell model, is used to describe the stress relaxation of grain boundaries, leading to an inverse Hall–Petch relation of the yield strength for the NC material as a function of the grain size, following the relation $\sigma = \sigma_{am.}(1 + g(d/w-1))$. The results are compared with the experimental data of Cu and Ni over entire ranges of grain sizes from micrometers to several nanometers, indicating that the conventional Hall–Petch relation works for $d > d_c$, while the aforementioned inverse Hall–Petch relation can be used to fit the experimental data for $d \leq d_c$. A new expression is proposed to describe the steady-creep rates of NC materials with grain sizes less than d_c. Compared with the Coble creep, the model indicates a smaller grain-size exponent for the creep of NC materials, as suggested by molecular-dynamic computer simulations.

ACKNOWLEDGMENTS

The authors GJ, HC, and PK are grateful for the financial support by the National Science Foundation International Materials Institutes (IMI) Program, with Dr. Carmen Huber as the Director. EJL gratefully acknowledges the financial support of the United States Army Research Office Grant No. DAAD19-03-1-0020.

APPENDIX

A shear stress is developed at the interfaces between the grain interior and gain-boundary layer, which depends on the position, with a maximum at one end of the grain interior decreasing gradually toward zero at the midpoint. The value of the shear stress also depends on its direction. Therefore, this is a very complicated situation. For simplicity, it is assumed that the shear stress is constant at all directions throughout the interfaces. Assuming a spherical shape of grains (Figure A1), a force balance requires

$$F = \int_0^{\frac{\pi}{2}} \tau_b r^2 \cos\beta \, d\beta \int_0^{\frac{\pi}{2}} \cos\alpha \, d\alpha = \frac{4\pi r^2}{8} \sigma_l \quad [A1]$$

Therefore,

$$\sigma_l = \frac{2}{\pi} \tau_b \quad [A2]$$

In the case of the hexagonal grains (Figure A2),

$$\sigma_l = 1.75\tau_b \quad [A3]$$

and for the cubic grains (not shown),

$$\sigma_l = 2\tau_b \quad [A4]$$

Therefore, the geometric factor g_2 in Eq. [8] is $2/\pi$ for spherical grains, 1.75 for hexagonal grains, and 2 for cubic grains, implying that geometric factor relates to the shape of a grain, although this may not represent the absolute value.

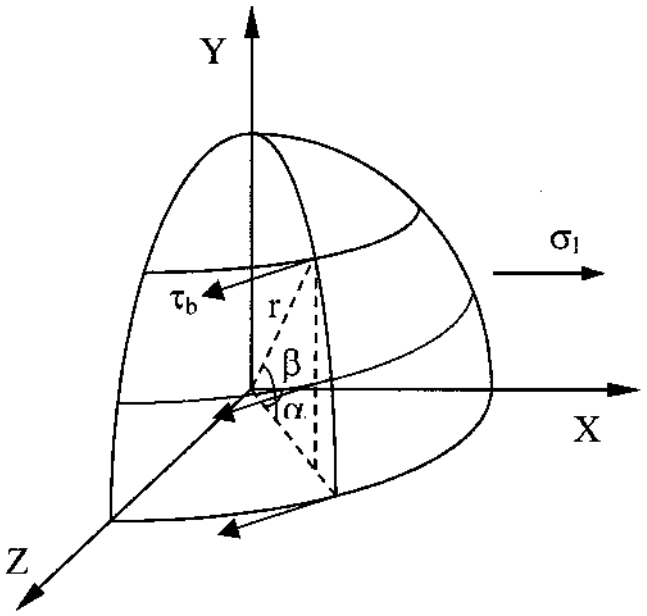

Fig. A1—A tensile stress, σ_l, is built up in a spherical grain interior with a radius of r, due to a shear stress of τ_b.

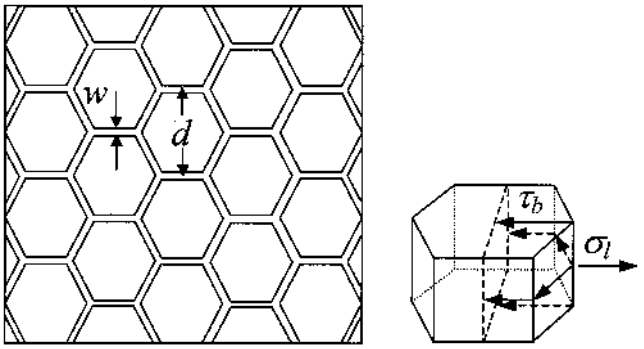

Fig. A2—A NC material consisting of a hexagonal grain with a grain size of d and a grain-boundary width of w.

REFERENCES

1. J.C.M. Li: *Acta Metall.*, 1960, vol. 8, pp. 296-304.
2. J.C.M. Li: *J. Appl. Phys.*, 1966, vol. 32, pp. 525-41.
3. E.O. Hall: *Proc. Phys. Soc. London*, 1951, vol. B64, pp. 747-53.
4. N.J. Petch: *J. Iron Steel Inst.*, 1953, vol. 174, pp. 25-28.
5. H. Gleiter: *Acta Mater.*, 2000, vol. 48, pp. 1-29.
6. K.S. Kumar, H. Van Swygenhoven, and S. Suresh: *Acta Mater.*, 2003, vol. 51, pp. 5743-74.
7. V. Yamakov, D. Wolf, S.R. Phillpot, and H. Gleiter: *Acta Mater.*, 2002, vol. 50, pp. 61-73.
8. T.R. Mallow and C.C. Koch: *Acta Mater.*, 1997, vol. 45, pp. 2177-86.
9. G.W. Nieman, J.R. Weertman, and R.W. Siegel: *J. Mater. Res.*, 1991, vol. 6, pp. 1012-27.
10. J.R. Weertman: *Mater. Sci. Eng.*, 1993, vol. A166, pp. 161-67.
11. T.G. Nieh and J. Wadsworth: *Scripta Metall. Mater.*, 1991, vol. 25, pp. 955-59.
12. J. Schiotz, F.D. Di Tolla, and K.W. Jacobsen: *Nature*, 1998, vol. 391, pp. 561-63.
13. J. Schiotz and K.W. Jacobsen: *Science*, 2003, vol. 301, pp. 1357-59.
14. V. Yamakov, D. Wolf, S.R. Phillpot, A.K. Mukherjee, and H. Gleiter: *Nature Mater.*, 2004, vol. 3, pp. 43-47.
15. P.G. Sanders, J.A. Eastman, and J.R. Weertman: *Acta Mater.*, 1997, vol. 45, pp. 4019-25.
16. E. Ma: *Scripta Mater.*, 2003, vol. 49, pp. 663-68.
17. H.J. Fecht and W.L. Johnson: *Nature*, 1988, vol. 334, pp. 50-51.

18. A.H. Chokshi, A. Rosen, J. Karch, and H. Gleiter: *Scripta Metall.*, 1989, vol. 23, pp. 1679-84.
19. C.A. Schuh, T.G. Nieh, and T. Yamasaki: *Scripta Mater.*, 2002, vol. 46, pp. 735-40.
20. C.A. Schuh, T.G. Nieh, and H. Iwasaki: *Acta Mater.*, 2003, vol. 51, pp. 431-43.
21. K.J. Van Vliet, S. Tsikata, and S. Suresh: *Appl. Phys. Lett.*, 2003, vol. 83, pp. 1441-43.
22. R. Scattergood and C.C. Koch: *Scripta Metall. Mater.*, 1992, vol. 27, pp. 1195-200.
23. H. Hahn, P. Mondal, and K.A. Padmanabhan: *Nano-Struct. Mater.*, 1997, vol. 9, pp. 603-06.
24. V.G. Gryaznov, M.Y. Gutkin, A.E. Romanov, and L.I. Trusov: *J. Mater. Sci.*, 1993, vol. 28, pp. 4359-65.
25. D.A. Konstantinidis and E.C. Aifantis: *Nano-Struct. Mater.*, 1998, vol. 10, pp. 1111-18.
26. N. Wang, Z. Wang, K.T. Aust, and U. Erb: *Acta Mater.*, 1995, vol. 43, pp. 519-29.
27. H. Conrad and J. Narayan: *Scripta Mater.*, 2000, vol. 42, pp. 1025-30.
28. H.S. Kim, Y. Estrin, and M.B. Bush: *Acta Mater.*, 2000, vol. 48, pp. 493-504.
29. R.A. Masumura, M.P. Hazzledine, and C.S. Pande: *Acta Mater.*, 1998, vol. 46, pp. 4527-34.
30. H.H. Fu, D.J. Benson, and M.A. Meyers: *Acta Mater.*, 2001, vol. 49, pp. 2567-82.
31. A.A. Fedorov, M.Y. Gutkin, and I.A. Ovid'ko: *Scripta Mater.*, 2002, vol. 47, pp. 51-55.
32. R.L. Coble: *J. Appl. Phys.*, 1963, vol. 34, pp. 1679-82.
33. H. Hahn and K.A. Padmanabhan: *Philos. Mag. B*, 1998, vol. 77, pp. 207-17.
34. M.Yu. Gutkin, I.A. Ovid'ko, and C.S. Pande: *Rev. Adv. Mater. Sci.*, 2001, vol. 2, pp. 80-92.
35. F.R.N. Nabarro: *Report on Conf. on the Strength of Solids*, Physical Society, London, 1948, pp. 75-84.
36. C. Herring: *J. Appl. Phys.*, 1950, vol. 21, pp. 437-50.
37. V. Yamakov, D. Wolf, M. Salazar, S.R. Phillpot, and H. Gleiter: *Acta Mater.*, 2001, vol. 49, pp. 2713-22.
38. H. Gleiter: *Prog. Mater. Sci.*, 1989, vol. 33, pp. 223-315.
39. X. Zhu, R. Birringer, U. Gonser, and H. Gleiter: *Appl. Phys. Lett.*, 1987, vol. 50, pp. 472-74.
40. G.J. Thomas, R.W. Siegel, and J.A. Eastman: *Scripta Metall. Mater.*, 1990, vol. 24, pp. 201-06.
41. H. Van Swygenhoven, D. Farkas, and A. Caro: *Phys. Rev.*, 2000, vol. B62, pp. 831-38.
42. A. Hasnauui, H. Van Swygenhoven, and P.M. Derlet: *Acta Mater.*, 2002, vol. 50, pp. 3927-39.
43. V. Yamakov, D. Wolf, S.R. Phillpot, A.K. Mukherjee, and H. Gleiter: *Nature Mater.*, 2002, vol. 1, pp. 45-48.
44. P. Keblinski, S.R. Phillpot, D. Wolf, and H. Gleiter: *Acta Mater.*, 1997, vol. 45, pp. 987-98.
45. P. Keblinski, D. Wolf, S.R. Phillpot, and H. Gleiter: *Scripta Mater.*, 1999, vol. 41, pp. 631-36.
46. J.H. He, H.W. Sheng, P.J. Schilling, C.L. Chien, and E. Ma: *Phys. Rev. Lett.*, 2001, vol. 86, pp. 2826-29.
47. J.H. Zhang and Y.S. Zhao: *Nature*, 2004, vol. 430, pp. 332-35.
48. H. Furuichi, E. Ito, Y. Kanno, S. Watanabe, T. Katsura, and N. Fujii: *J. Non-Cryst. Solids*, 2001, vol. 279, pp. 215-18.
49. J.M. Soler, M.R. Beltran, K. Michaelian, I.L. Garzon, P. Ordejon, D. Sanchez–Portal, and E. Artacho: *Phys. Rev.*, 2000, vol. B61, pp. 5771-80.
50. J. Lu and J.A. Szpunar: *Phil. Mag.*, 1997, vol. A75, pp. 1057-66.
51. T.M. Brown and J.B. Adams: *J. Non-Cryst. Solids*, 1995, vol. 180, pp. 275-84.
52. O.R. De La Fuente and J.M. Soler: *Phys. Rev. Lett.*, 1998, vol. 81, pp. 3159-62.
53. H. Van Swygenhoven and A. Caro: *Phys. Rev.*, 1998, vol. B58, pp. 11246-351.
54. B.J. Edwards, A.N. Beris, and V.G. Mavrantzas: *J. Rheol.*, 1996, vol. 40, pp. 917-42.
55. K. Nitta and K. Suzuki: *Macromol. Theory Simul.*, 1999, vol. 8, pp. 254-59.
56. G.G. Stokes: *Math. Physical Papers*, 1880, vol. 1, pp. 38-51.
57. A. Einstein: *Brownian Movement*, 1956.
58. G. Tarjus and D. Kivelson: *J. Chem. Phys.*, 1995, vol. 103, pp. 3071-73.
59. F.H. Stillinger: *Science*, 1995, vol. 267, pp. 1935-39.
60. U. Geyer, W.L. Johnson, S. Schneider, Y. Qiu, T.A. Tombrello, and M.P. Macht: *Appl. Phys. Lett.*, 1996, vol. 69, pp. 2492-94.
61. L. Angelani, G. Parisi, G. Ruocco, and G. Viliani: *Phys. Rev. E*, 2000, vol. 61, pp. 1681-91.
62. J. Horvath, R. Birringer, and H. Gleiter: *Sol. State Commun.*, 1987, vol. 62, pp. 319-22.
63. E. Arzt: *Acta Mater.*, 1998, vol. 46, pp. 5611-26.
64. V. Bata and E.V. Pereloma: *Acta Mater.*, 2004, vol. 52, pp. 657-65.
65. K. Hayashi and H. Etoh: *Metall. Trans. JIM*, 1989, vol. 309, pp. 925-31.
66. P.G. Sanders, J.A. Eastman, and J.R. Weertman, in: *Processing and Properties of Nanocrystalline Materials*, R. Suryanarayana, J. Singh, and F.H. Fores, eds., TMS, Warrendale, PA, 1996, pp. 397-405.
67. R. Suryanarayana, C.A. Frey, S.M.L. Sastry, B.E. Waller, S.E. Bates, and W.E. Buhro: *J. Mater. Res.*, 1996, vol. 11, pp. 439-48.
68. F. Ebrahimi, G.R. Bourne, M.S. Kelly, and T.E. Matthews: *Nano-Struct. Mater.*, 1999, vol. 11, pp. 343-50.
69. F. Dalla Torre, H. Van Swygenhoven, and M. Victoria: *Acta Mater.*, 2002, vol. 50, pp. 3957-70.
70. A.M. El-Sherik, U. Erb, G. Palumbo, and K.T. Aust: *Scripta Metall. Mater.*, 1992, vol. 27, pp. 1185-88.
71. T. Yamasaki: *Scripta Mater.*, 2001, vol. 44, pp. 1497-502.
72. H.S. Chen: *J. Appl. Phys.*, 1978, vol. 49, pp. 462-63.
73. G.J. Fan, X.P. Song, M.X. Quan, and Z.Q. Hu: *Mater. Sci. Eng.*, 1997, vol. A231, pp. 111-16.
74. B. Cai, Q.P. Kong, L. Lu, and K. Lu: *Scripta Mater.*, 1999, vol. 41, pp. 755-59.
75. N. Wang, Z. Wang, K.T. Aust, and U. Erb: *Mater. Sci. Eng.*, 1997, vol. A237, pp. 150-58.
76. W.M. Yin, S.H. Whang, R. Mirshams, and C.H. Xiao: *Mater. Sci. Eng.*, 2001, vol. A301, pp. 18-22.
77. R. Rodriguez, R.W. Hayes, P.B. Berbon, and E.J. Lavernia: *Acta Mater.*, 2003, vol. 51, pp. 911-29.
78. R.W. Hayes, V. Tellkamp, and E.J. Lavernia: *J. Mater. Res.*, 2000, vol. 15, pp. 2215-22.
79. P.M. Derlet and H. Van Swygenhoven: *Scripta Mater.*, 2002, vol. 47, pp. 719-24.
80. H. Van Swygenhoven and A. Caro: *Appl. Phys. Lett.*, 1997, vol. 71, pp. 1652-54.
81. M.F. Ashby: *Scripta Metall.*, 1969, vol. 3, pp. 837-42.
82. E. Arzt, M.F. Ashby, and R.A. Verall: *Acta Metall.*, 1983, vol. 31, pp. 1977-89.
83. P.G. Sanders, M. Rittner, E. Kiedaisch, J.R. Weertman, H. Kung, and Y.C. Lu: *Nano-Struct. Mater.*, 1997, vol. 9, pp. 433-40.
84. I. Kaur, W. Gust, and L. Kozma: *Handbook of Grain and Interphase Boundary Diffusion Data*, Ziegler Press, Stuttgart, 1989.